ARTICLE

Bioconvection Cross Diffusion Effects on MHD Flow of Nanofluids over Three Different Geometries with Melting

Tahir Kamran, Muhammad Imran[*], Muhammad N. Naeem and Mohsan Raza

Department of Mathematics, Government College University Faisalabad, Faisalabad, 38000, Pakistan
[*]Corresponding Author: Muhammad Imran. Email: drmimranranchaudhry@gmail.com

ABSTRACT

Currently, nanofluid is a hot area of interest for researchers. The nanofluid with bioconvection phenomenon attracted the researchers owing to its numerous applications in the field of nanotechnology, microbiology, nuclear science, heat storage devices, biosensors, biotechnology, hydrogen bomb, engine of motors, cancer treatment, the atomic reactor, cooling of devices, and in many more. This article presents the bioconvection cross-diffusion effects on the magnetohydrodynamic flow of nanofluids on three different geometries (cone, wedge, and plate) with mixed convection. The temperature-dependent thermal conductivity, thermal diffusivity, and Arrhenius activation energy applications are considered on the fluid flow with melting phenomenon. The flow is analyzed under thermal and solutal Robin's conditions. The problem is formulated in the mathematical formulation of partial differential equations (PDEs). The similarity transformations are applied to diminish the governing non-linear coupled boundary value problems into higher-order non-linear ordinary differential equations (ODEs). The resulting expressions/equation numerically tackled utilizing the famous bvp4c package by MATLAB for various interesting parameters. The results were physically and numerically calculated through graphics and tables for the velocity field, energy distribution, nanoparticles concentration, and microorganisms profile for numerous parameters. From the obtained results, we discern that the transfer of heat and mass coefficient is high over a plate and cone in the flow, respectively. The velocity profile is reduced via a larger magnetic parameter. Temperature-dependent thermal conductivity enhances the thermal field. Larger thermophoresis enhanced the concentration of nanoparticles. The microorganisms' Biot number boosts the microorganism's profile.

KEYWORDS

MHD; nano-fluids; bioconvection; heat flux; MATLAB

Nomenclature

C	Concentration of Nanomaterials, mol L^{-1}
Pe	Peclet Number
α	Half Angle of Cone, Radian
Ω	Full Angle of Wedge, Radian
D_B	Brownian Diffusion Coefficient, m^2 s^{-1}

a, b, c	Real Constants
D_T	Thermophoresis Diffusion Coefficient, $m^2\ s^{-1}$
G_r	Grashof Number
W_C	Cell Swimming Speed, $m\ s^{-1}$
Ω_1	Thermal Biot Number
ξ	Stream Velocity Function, m^2/sec
s, q, n	Energy, Concentration, and Bioconvection Parameters
N	Concentration of Microorganisms, m^{-3}
β_t	Volumetric Thermal Expansion Coefficients, 1/Kelvin
β_C	Volumetric Concentration Expansion Coefficients 1/mol L^{-1}
β_n	Volumetric Microorganisms Expansion Coefficients, $1/m^3$
D	Microorganisms Coefficient, $m^2\ s^{-1}$
E_a	Activation Energy, J
M	Magnetic Parameter
Ω_2	Solutal Biot Number
λ	Mixed Convection Parameter
Ω_3	Microorganism Biot Number
ε_1	Temperature Dependent Thermal Conductivity
T	Temperature of Nanoliquid, K
Rd	Radiation Parameter
u, v	Velocity Component, $m\ s^{-1}$
Pr	Prandtl Number
x y	Coordinates System, m
Nc	Bioconvection Rayleigh Number
h_f	Convective Heat Transfer Coefficient, $Wm^2\ K^{-1}$
Nt	Thermophoresis Parameter
ε_2	Concentration Diffusivity
Ma	Melting Parameter
Nb	Brownian Motion Parameter
$K(T)$	Variable Thermal Conductivity
Le	Lewis Number
$D(C)$	Variable Mass Diffusivity
δ	Temperature Difference Parameter
δ_1	Microorganisms Difference Parameter
σ^{**}	Chemical Reaction Parameter
Cf	Skin Friction Coefficient
Me	Melting Parameter
Sn	Local Density Number of Microorganisms
Nu	Local Nusselt Number
S_h	Local Sherwood Number
g	Gravitation Force, m/sec^2
l	Characteristic Length
r	Radius of Cone, m
(ρc_p)	Heat Capacitance, $Jm^{-3}\ K^{-1}$
ρ_f	Density of Nanoliquid, $kg\ m^{-3}$

Subscript

w	Wall
f	Fluid
0	Ambient
∞	Free–Stream

1 Introduction

Magnetohydrodynamics (MHD) has a vital role in several flow phenomena, including industry. The MHD is applied in various fields, including multidisciplinary technological areas like biochemical manufacturing heat transfer, automotive sector, ceramic technology, aerodynamic performance, metallurgical technology, mental operating techniques, and fluid dynamics. Magnetohydrodynamic initiation changes the flow field's preferred direction by fluctuating boundary layer configuration flow. Electromagnetic fields play an important role in convection mechanisms like metallic casting, material processing fields, and nuclear reactor control plants. Zheng et al. [1] investigated the heat transformation in the two-dimensional flow of magnetohydrodynamic (MHD) by considering temperature and velocity slip effects through a shrinking porous surface. It was stated that the thermal boundary layer flow declined to owe to an increase in the shrinking parameters. The heat transmission and magnetohydrodynamic flow through the porous plate and shrinking surface were studied by Chauhan et al. [2]. The central concept was that the cooling rate was controlled by the electromagnetic number and suction parameter over channels bounded. Attia [3] examined the different physiological properties of the unsteady MHD Couette flowing heat exchange in a dusty fluid flow with variable viscosity. Kumar et al. [4] explored mass and heat transport across a vertical plate under the cross-diffusion impact in radiative mixed convective cases of magneto-hydrodynamic fluid flow. The fluid movement increased with an increase in both the buoyancy force variables and the mixed convection parameter. Ibrahim et al. [5–7] observed heat exchange and MHD boundary layer nanofluid flow via vertical surfaces and a non–isothermal expanding surface using the similarity transformation technique. Ibrahim et al. [8,9] described nanoparticles' MHD boundary layer flow through a stretched surface, influenced by double stratification and diffusion. Muhammad et al. [10] discussed the Eyring- Powell nanofluid with thermal radiation effects. Waqas et al. [11] checked the melting effects in a modified second-grade nanofluid. Danish et al. [12] explore the EMHD effects in Williamson nanofluid with activation energy and nonlinear thermal radiation. Waqas et al. [13] analyzed the flow and heat transfer improvement in radiative hybrid nanofluid flow across the disk. Mabood et al. [14] analyzed radiative nanofluid across the thin needle.

Several investigators studied heat transfer due to its various applications in applied technologies, manufacturing, and refrigeration. Thermally conductive fluid has subsequently become a common research topic for scientists. Nanotechnology is becoming a subject of significant interest in manufacturing and engineering for investigators as its requirement grows in industrial sectors. Non-Newtonian fluids are now a big subject for scientists and physiologists [15–17]. Moreover, the world is experiencing an energy problem because of global heating and pollution. As a result, researchers are working to develop new heat transfer techniques to make improvements that can be justified. Nanotechnology is one of the researchers' most recent techniques to help alleviate energy shortages. Choi et al. [18] introduced the nanofluids, and they have since achieved boundless attention. Nanofluids are the most using coolants in the industry. The thermal properties of a combination of nanometer-sized particles immersed in a fluid identified as nanofluids or base fluids improved due to the involvement of these nanomaterials. Buongiorno [19] explored how to augment the convection rate of heat transformation in two significantly slip situations: thermophoresis diffusion and Brownian motion behavior.

Bioconvection occurs because the microorganisms are denser than water; therefore, a motile gyrotactic microorganism moves upwardly in water. The production of the base fluid increased as the dynamically self-propelled motile gyrotactic microorganisms moved in a particular direction. Bioconvection is used in various areas, including fertilizer, biofuel, and manufacturing systems.

Nanofluid bioconvection is considered for density stratified as well as patron formation due to nanomaterials apprentice, buoyancy forces, including microorganisms. Kuznetsov [20] reported that bioconvection in nanofluids is expected to occur if the concentration of nanoparticles is small so that nanoparticles do not cause any significant increase in the viscosity of the base fluid. Ali et al. [21] studied the bio-convectional of micropolar nanofluids in water-based concentrations containing microorganisms and nanoparticles. Nayak et al. [22] scrutinized the effects of velocity, temperature, solutal and motile gyrotactic microorganism slip lying on the biologically neutral Casson nano liquid flow across an exponential expanding electro- magnetic surface with chemical effects. Khan et al. [23] analyzed the bioconvection impact in the rheological nano liquid stress coupled with Arrhenius activation energy and Wu's slip with magnetic properties. The bioconvection motion of nanofluids caused by gyrotactic motile microorganisms was mentioned by Kotha et al. [24]. The motile gyrotactic microorganisms and thermal radiation for the chemical bonded bio-convectional flow of tangent hyperbolic nanofluids were reported by Al-Khaled et al. [25]. For dispersing gyrotactic motile microorganisms and the density of gyrotactic microorganisms, including velocity profiles, are declining, the Schmidt number is performed by Makinde et al. [26]. The bioconvection Rayleigh number and the local thermal Grashof number are diminishing functions for motile gyrotactic microorganism diffusion is evaluated by Makinde et al. [27]. Saleem et al. [28] examined the density computed for motile gyrotactic microorganisms shrinks above the Peclet number under the bio convection effect. Waqas et al. [29] examined bioconvection effects on modified second-grade nanofluid microorganisms. Chu et al. [30] discussed the modified diffusion in tangent hyperbolic nanofluid under the bioconvection phenomenon. Many researchers [31–38] explore the bioconvection phenomenon in nanofluid flow.

Furthermore, affiliation with a related domain that is closely suitable in real life has a significant impact. Because of their significance in multiple fields of technology agriculture, including manufacturing applications, the flows generated through a wedge, cone, and vertical plate have gotten a lot of attention. Vajravelu et al. [39] developed a mathematical mechanism for transmitting heat reacting to flow via a cone and wedge. Chamkha [40] explained that the heat source parameter improved the local Nusselt number by considering the flow, including porosity. Many investigators in various fields, specifically fluid dynamics, used wedge as the geometry in their experiments because they implemented the above–mentioned work. Khan et al. [41] observed the flow of a nano liquid throughout a rotating wedge under the chemical process, including thermal radiation. Interestingly, fluid dynamics scientists are currently considering the action of heat transformation over wedge flows.

Whereas mass and heat transport occurs continuously in a moveable fluid. Compared to the Dufour effect, the Soret effect is negligible in fluids. Numerous researchers have reported cross-diffusion influences in boundary layer flow in recent decades. Abd El-Aziz [42] discussed the consequences of Dufour, radiation, Soret parameters, and Magnetohydrodynamic over a porous sheet that is often stretched. He discovered that the Dufour and Soret parameters have an important impact on temperature, momentum, and assemble distributions. Eckert et al. [43] and Mortimer et al. [44] have addressed a variety of flow events, including those in geophysics, where thermal diffusion and diffusion thermo consequences are highly suspected. Thermal–diffusion and Diffusion–thermo are imperative when density differences occur in the fluid flow, according to Devi et al. [45]. Thermal–diffusion and Diffusion–thermo influences have been most significant for interfering molecular weight gases in binary processes frequently confronted in chemical technology mechanisms.

MATLAB is an essential software tool for numerically solving and comparing the outcomes of various models, including physics, technology, and a variety of others. The variable flowing and thermal characteristics when a decelerating rotating disc is modified scrutinized by Rafiq et al. [46]. The consequence of thermal conductivity and the variable viscosity overheat transmission rates and drag was discovered in a two-way analysis for a numerical solution using Matlab-bvp4c and R-K shooting methods.

The study of bioconvection in nanofluid is beneficial in different fields like biofuels cells, biotechnology, bioengineering, oil refineries, biofuels, and agriculture engineering. To the author's best knowledge, no studies have yet reported analyzing bioconvections for the heat and mass transfer of the MHD flow with cross-diffusion impacts by considering three different geometries by considering the thermal and solutal Robin's conditions. So, we filled this gap with the assistance of the above-cited studies. The prime motive of this study is to investigate the consequences of the occurrence of motile microorganisms on nanofluid flow with thermal radiation, activation energy, and melting phenomena past the geometries cone, wedge, and the plate. Appropriate similarity transformations are used to convert the PDEs into ODEs, and these equations are solved by numerical technique through shooting methods using bvp4c solver. Outcomes are exposed graphically and conferred numerical values for various physical parameters.

2 Mathematical Development of the Problem

Assume an incompressible, convective, time independent, laminar MHD flow over geometries of three different shapes like cone, wedge and plate. The melting mechanism is measured. In the plane xy, we considered surface of the body is measured by x and normally outward to the surface measured by y. Fig. 1 shows that strength B_0 of transverse electro–magnetic field is applying perpendicularly along the flow on surface of the geometry. The half angle of cone represented by α and full angle of wedge represented by Ω, the cone radius shown by r. Let ξ be the stream velocity function. The temperature of fluid, concentration and bioconvection near the plate is presented as $T_w = T_0 + ax^s$, $C_w = C_0 + bx^q$ and $N_w = N_0 + cx^n$, here (a, b and c) are real constants, (s, q and n) are the energy, concentration, and bioconvection parameters for wall (the energy, concentration, and bioconvection over wall is constant when $(s = q = n = 0)$), $(T_0, C_0$ and $N_0)$ are the ambient temperature, concentration and bioconvection. Mixed convection heat flux, cross diffusion impacts are included in the given problem.

For the above considered problem the basic coupled nonlinear dimensional equations are given below [47]:

$$\frac{\partial}{\partial x}\left(r^m \frac{\partial \xi}{\partial y}\right) - \frac{\partial}{\partial y}\left(r^m \frac{\partial \xi}{\partial x}\right) = 0, \tag{1}$$

$$\frac{\partial \xi}{\partial y}\frac{\partial^2 \xi}{\partial x \partial y} - \frac{\partial \xi}{\partial x}\frac{\partial^2 \xi}{\partial y^2} = v\frac{\partial^3 \xi}{\partial y^3} + (\beta_t(T - T_\infty) + \beta_c(C - C_\infty) + \beta_n(N - N_\infty))g\cos\alpha - \frac{\sigma\beta_0^2}{\rho}\frac{\partial \xi}{\partial y}, \tag{2}$$

$$\frac{\partial \xi}{\partial y}\frac{\partial T}{\partial x} - \frac{\partial \xi}{\partial x}\frac{\partial T}{\partial y} = \frac{k}{\rho c_p}\frac{\partial^2 T}{\partial y^2} + \frac{1}{(\rho c_p)_f}\frac{\partial}{\partial y}\left(K(T)\frac{\partial T}{\partial y}\right) + \tau\left[D_B\frac{\partial C}{\partial y}\frac{\partial T}{\partial y} + \frac{D_T}{T_\infty}\left(\frac{\partial T}{\partial y}\right)^2\right], \tag{3}$$

$$\frac{\partial \xi}{\partial y}\frac{\partial C}{\partial x} - \frac{\partial \xi}{\partial x}\frac{\partial C}{\partial y} = \frac{1}{(\rho c_p)_f}\frac{\partial}{\partial y}\left(D(C)\frac{\partial C}{\partial y}\right) + D_B\frac{\partial^2 C}{\partial y^2} + \frac{D_T}{T_\infty}\left(\frac{\partial^2 T}{\partial y^2}\right)$$

$$-K_1 r^2 (C - C_\infty)\left(\frac{T}{T_\infty}\right)^2 \exp\left(\frac{-E_a}{\kappa T}\right),$$

(4)

$$\frac{\partial \xi}{\partial y}\frac{\partial N}{\partial x} + \frac{\partial \xi}{\partial x}\frac{\partial N}{\partial y} + \left[\frac{\partial}{\partial y}\left(N\frac{\partial C}{\partial y}\right)\right]\frac{bW_c}{(C_w - C_\infty)} = D_m\frac{\partial}{\partial y}\left(\frac{\partial N}{\partial y}\right).$$

(5)
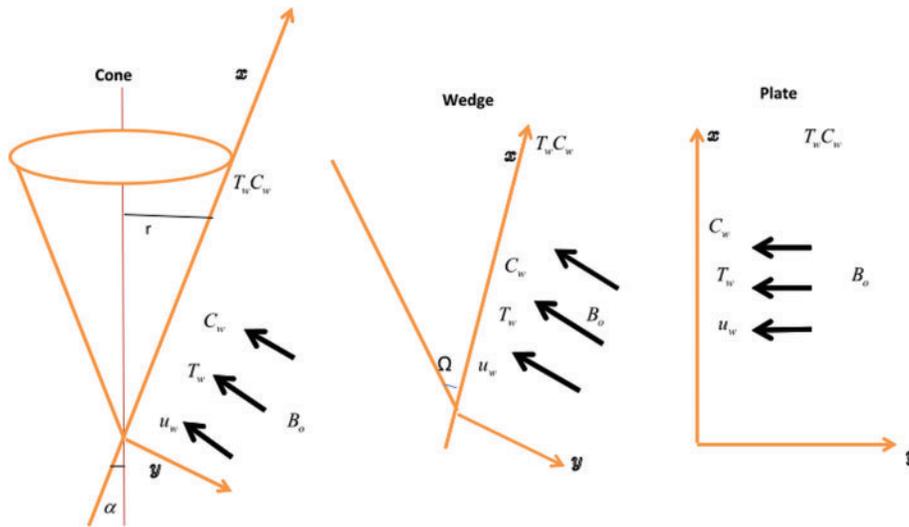
Figure 1: Schematic flow with coordinate system

The applied boundaries conditions are [48]

$$u(x, 0) = u_w = vx/l^2, v(x, 0) = 0, \quad k\frac{\partial T}{\partial y} = h_f(T_w - T),$$

$$D_B\frac{\partial C}{\partial y} = h_g(C_w - C), D_m\frac{\partial N}{\partial y} = h_n(N_w - N),$$

$$u \to 0, T \to T_\infty, C \to C_\infty, N \to N_\infty \quad as \quad y \to \infty.$$

(6a)

$$-k\frac{\partial T}{\partial y}\bigg|_{y=0} = \rho\left[\lambda_0 + (T_m - T_0)c_s\right]$$

(6b)

(1) If $m = 0$ and $\alpha \neq 0$ then flow problem for wedge.
(2) If $m = 1$ and $\alpha \neq 0$ then flow problem for cone.
(3) If $m = 0$ and $\alpha = 0$ then flow problem for plate.

Introduced the suitable similarities variables

$$\zeta = yl^{-1}, u = vxl^{-2}\frac{\partial f}{\partial \zeta}, v = -v(m+1)l^{-1}f(\zeta),$$

$$\theta(\zeta)(T_w - T_\infty) + T_\infty = T, \phi(\zeta)(C_w - C_\infty) + C_\infty = C, \tag{7}$$

$$\chi(\zeta)(N_w - N_\infty) + N_\infty = N.$$

Transformation equations are as follows:

$$\frac{d^3f}{d\zeta^3} + (m+1)f\frac{d^2f}{d\zeta^2} - \left(\frac{df}{d\zeta}\right)^2 - M\frac{df}{d\zeta} + \lambda(\theta + Gr\phi + Nc\chi)\cos\alpha = 0, \tag{8}$$

$$(1+\varepsilon_1\theta)\frac{d^2\theta}{d\zeta^2} + \varepsilon_1\left(\frac{d\theta}{d\zeta}\right)^2 + \Pr\left(Nb\frac{d\theta}{d\zeta}\frac{d\phi}{d\zeta} + Nt\left(\frac{d\theta}{d\zeta}\right)^2\right)$$
$$+\Pr\left((m+1)f\frac{d\theta}{d\zeta} - s\frac{df}{d\zeta}\theta\right) = 0, \tag{9}$$

$$(1+\varepsilon_2\phi)\frac{d^2\phi}{d\zeta^2} + \varepsilon_2\left(\frac{d\phi}{d\zeta}\right)^2 + LePr\left((m+1)f\frac{d\phi}{d\zeta} - s\frac{df}{d\zeta}\phi\right) + \frac{Nt}{Nb}\frac{d^2\theta}{d\zeta^2}$$
$$-Le\Pr\sigma^{**}(1+\delta\theta)^n\phi\exp\left(-\frac{E}{1+\delta\theta}\right) = 0, \tag{10}$$

$$\frac{d^2\chi}{d\zeta^2} + Lb\left((m+1)f\frac{d\chi}{d\zeta} - s\frac{df}{d\zeta}\chi\right) - Pe\left[\frac{d^2\phi}{d\zeta^2}(\chi+\delta_1) + \frac{d\chi}{d\zeta}\frac{d\phi}{d\zeta}\right] = 0, \tag{11}$$

where s representing the temperature parameter.

The dimension-less conditions are as follows:

$$Me\theta'(0) + \Pr f(0) = 0, \frac{df}{d\zeta} = 1, \frac{d\theta}{d\zeta} = -\Omega_1(1-\theta(0)),$$
$$\frac{d\phi}{d\zeta} = -\Omega_2(1-\phi(0)) = 0, \frac{d\chi}{d\zeta} = -\Omega_3(1-\chi(0)) at \zeta = 0 \tag{12}$$

$$\frac{df}{d\zeta} = 0, \theta = 0, \phi = 0, \chi = 0 \, as \, \zeta \to 0. \tag{13}$$

In above equations M is the magnetic field, l is the characteristic length, λ is mixed convection parameter, Gr designed for Grashof number for concentration, Nc describe the Grashof number for microorganisms, Pr explain the Prandtl number, Nb demonstrate the Brownian motion, Nt illustrate the thermophoresis diffusion parameter, Lb confirm the bioconvection Lewis number, Pe represent the Peclet number, δ is the temperature difference parameter, microorganisms difference parameter denoted by δ_1 and thermal Biot number characterized by Ω_1, solutal Biot number indicated by Ω_2 and the microorganisms Biot number symbolized by Ω_3, ε_1 is the temperature dependent thermal conductivity, ε_2 denotes the Concentration diffusivity, σ^{**} denotes the chemical reaction parameter and melting parameter can be defined as Me.

$$M = \frac{\sigma_0 \beta_0^2 l^2}{\rho \nu}, \lambda = \frac{l^2 g \beta_t (T_w - T_\infty)}{\nu u_w}, Gr = \frac{l^2 g \beta_c (C_w - C_\infty)}{\nu u_w}, Nc = \frac{l^2 g B_n (N_w - N_\infty)}{\nu u_w},$$

$$\text{Pr} = \frac{\mu c_p}{k}, Nb = \frac{\tau D_B (C_w - C_\infty)}{\nu}, Nt = \frac{\tau D_T (T_w - T_\infty)}{\nu T_\infty}, Lb = \frac{\nu}{D_m}, \tag{14}$$

$$Pe = \frac{b W_c}{\nu}, \delta_1 = \frac{N_\infty}{N_w - N_\infty}, \Omega_1 = \frac{h_f}{k} l, \Omega_2 = \frac{h_g}{D_B} l, \Omega_3 = \frac{h_n}{D_M} l, Me = \frac{c_p (T_\infty - T_m)}{\lambda_0 + c_s (T_m - T_0)}.$$

The friction factor C_f, local Nusselt number Nu, local Sherwood number Sh and Sn defined as

$$C_f = \frac{C_f *}{\mu u_w} = - \frac{d^2 f}{d\zeta^2}\bigg|_{\zeta=0}, Nu = \frac{hl}{k(T_w - T_\infty)} = - \frac{d\theta}{d\zeta}\bigg|_{\zeta=o}, Sh = \frac{h_m l}{k(C_w - C_\infty)} = - \frac{d\phi}{d\zeta}\bigg|_{\zeta=0},$$

$$Sn = \frac{h_n l}{k(N_w - N_\infty)} = - \frac{d\chi}{d\zeta}\bigg|_{\zeta=0}. \tag{15}$$

3 Numerical Scheme

In this portion the nonlinear dimensionless ordinary differential equations with appropriate boundary conditions are solved numerically through the solver bvp4c package in computational MATLAB. The higher order ODEs are converted into linear one by introducing the following variables such as

$$f = p, \frac{df}{d\zeta} = p_1, \frac{d^2 f}{d\zeta^2} = p_2, \frac{d^3 f}{d\zeta^3} = p'_2,$$

$$\theta = p_3, \frac{d\theta}{d\zeta} = p_4, \frac{d^2 \theta}{d\zeta^2} = p'_4,$$

$$\phi = p_5, \frac{d\phi}{d\zeta} = p_6, \frac{d^2 \phi}{d\zeta^2} = p'_6, \tag{16}$$

$$\chi = p_7, \frac{d\chi}{d\zeta} = p_8, \frac{d^2 \chi}{d\zeta^2} = p'_8.$$

$$p'_2 = -(m+1)pp_2 + (p_1)^2 + Mp_1 - \lambda(p_3 + Grp_5 + Ncp_7)\cos\gamma, \tag{17}$$

$$p'_4 = \frac{-\varepsilon_1 (p_4)^2 - \text{Pr}(Nbp_4 p_6 + Nt(p_4)^2) - \text{Pr}((m+1)pp_4 - sp_1 p_3)}{(1 + \varepsilon_1 p_3)}, \tag{18}$$

$$p'_6 = \frac{-\varepsilon_2 (p_6)^2 - Le\text{Pr}((m+1)pp_6 - sp_1 p_5) - \frac{Nt}{Nb}p'_4 + Le\,\text{Pr}\,\sigma^{**}(1+\delta p_3)^n p_5 \exp\left(-\frac{E}{1+\delta p_3}\right)}{(1 + \varepsilon_2 p_5)}, \tag{19}$$

$$p'_8 = -Lb((m+1)pp_8 - sp_1p_7) + Pe[p'_6(p_7 + \delta_1) + p_8p_6], \tag{20}$$

With

$$Mep_4(0) + \Pr p(0) = 0, p_1 = 1, p_4 = -\Omega_1(1 - p_3(0)), p_6 = -\Omega_2(1 - p_5(0)) = 0,$$
$$p_8 = -\Omega_3(1 - p_7(0)) \, at \, \zeta = 0 \tag{21}$$

$$p_1 = 0, p_3 = 0, p_5 = 0, p_7 = 0 \, as \, \zeta \to 0. \tag{22}$$

4 Description of the Results

In this section all the results of graphs are embellished and created by using the computational software MATLAB–16a (bvp4c) solver. For the understanding of figures, we must have to know about the color of curves demonstrated. The black curve demonstrates for wedge, red for cone and blue for sheet. The iterations of effective goods parameters increased or decreased with their individual behaviors. In this segment the graphic outcome interoperate for the different values of different parameters, like $\Pr = 2.0$, $Pe = 0.1$, $E = 0.1$, $\varepsilon_2 = 0.1$, $Lb = 1.2$, $Le = 1.2$, $Nb = 0.1$, $Nt = 0.1$, $\Omega_1 = 0.1$, $\Omega_2 = 0.2$, $\Omega_3 = 0.1$, $M = 0.5$, $Nr = 0.1$, $Nc = 0.1$, $Me = 0.5$.

The influence of buoyancy ratio parameter Nr and velocity distribution f' is illustrated in Fig. 2. It is noticed from this figure that for the highest values of Nr, f' decreases (Fig. 3). Illustrates the fluctuation of the bioconvection Rayleigh number Nc with respect to the microorganism field with in the velocity profile f'. Such that the value of bioconvection Rayleigh number Nc increase due to the increased value of microorganism graph. The relationship between the buoyancy and viscosity is known as Rayleigh number within the fluids. The significant magnetic field parameter M against velocity distribution f' has been examined in Fig. 4. The velocity of the fluid decreased with the increased value of M. Once more this behavior is defined as the Hartmann number is interlinked with the occurrence of Lorentz force. Figs. 5–8 are examines the variation of Me on motile density profile χ, concentration profile φ, temperature profile θ and velocity profile f' respectively for three different geometries (wedge, cone and sheet). The fluctuation in Me reduces the motile density profile χ, concentration profile φ, temperature profile θ and velocity profile f'.
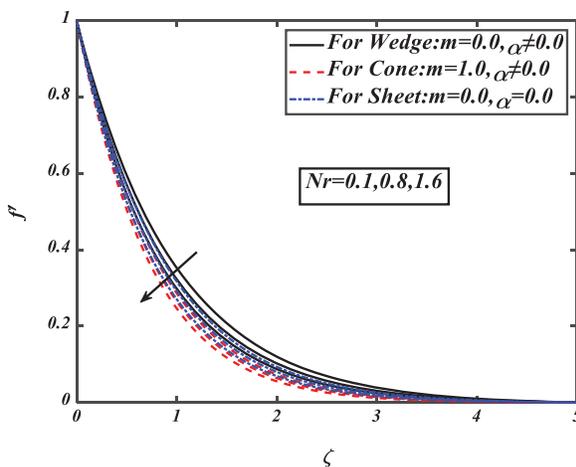
Figure 2: Pictogram of Nr over f'
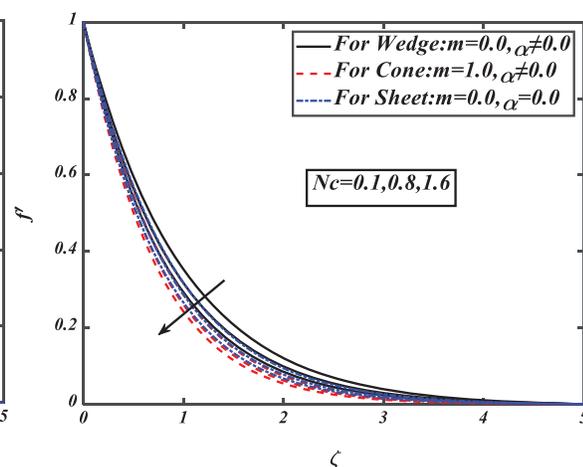
Figure 3: Pictogram of Nc over f'
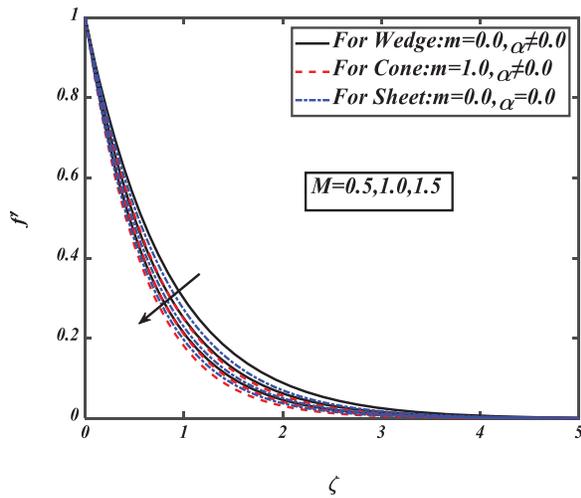
Figure 4: Pictogram of M over f'
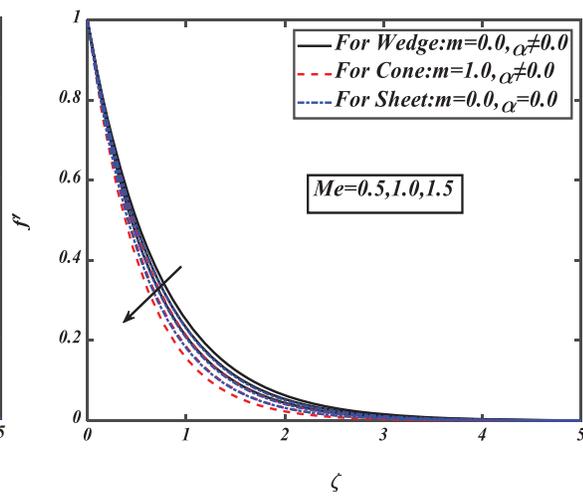
Figure 5: Pictogram of Me over f'
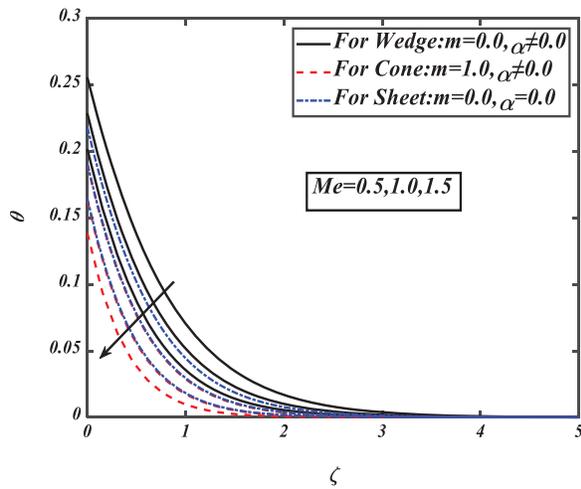
Figure 6: Pictogram of Me over θ
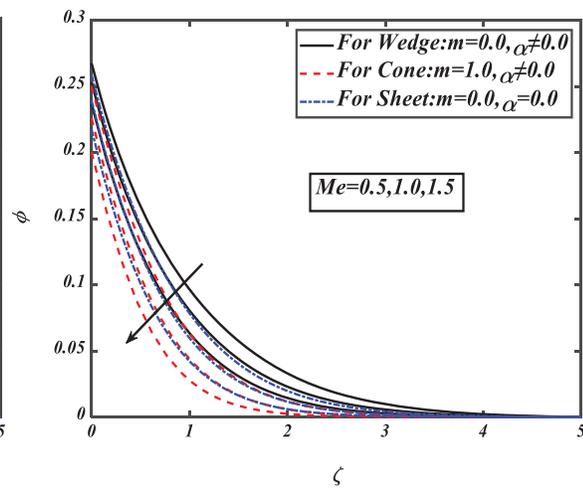
Figure 7: Pictogram of Me over ϕ

Fig. 9 illustrates the impact of the Prandtl number over temperature distribution respectively for different value of m for cone, wedge and sheet. Fig. 10 demonstrates the impact of thermal Biot number via temperature distribution for different geometries for several values of m and α. For cone $m = 1.0$ and for other two geometries its zero. Fig. 11 depicts that concentration is reduced via larger Prandtl number Pr. In Fig. 12 the activation energy E parameter is communicated for the nanoparticles volume distribution. In this graph when the value of E is increasing then the rate of reaction is decline due to higher temperature and greatest activation energy which develop the nanoparticles volume fraction. The concentration profile for ε_2 is deeply observed in the Fig. 13. Concentration dependent thermal diffusivity enhances the concentration field of nanoparticles. Fig. 14 analyzed the effect of Lewis number Le over concentration ϕ. The

decreasing in ϕ is noticed for demonstrative value of Le for three different geometries. The Le is defined to be the ratio of mass and thermal diffusivity. The ϕ is decreased for the higher value of Le in these geometries. Fig. 15 represented the variation of φ for the Brownian motion parameter Nb. The relationship between Nb and nanoparticles concentration is inverse. φ. From Fig. 16 the temperature distribution is upswing owing to the growing value of thermophoresis parameter Nt. For Nt the temperature profile improved, so the migration of particles from region to region exists as hot to cold region. Multi industrial processes use this concept now a days. The profile of concentration is increased for given value of Nt. The components of representational non–dimensional nanoparticles concentration ϕ is purposed through allotting unique values to Nt for three different geometries.
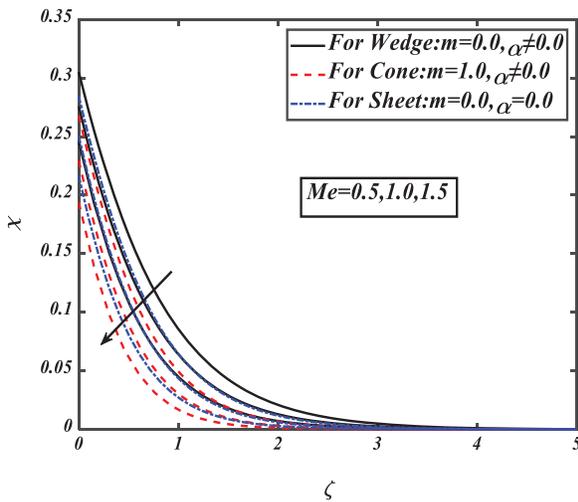
Figure 8: Pictogram of Me over χ
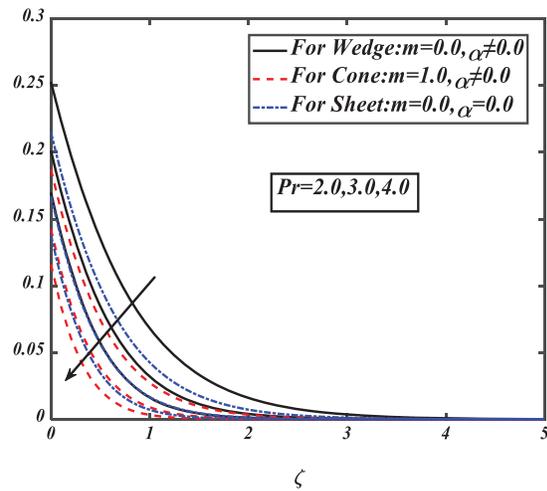
Figure 9: Pictogram of Pr over θ
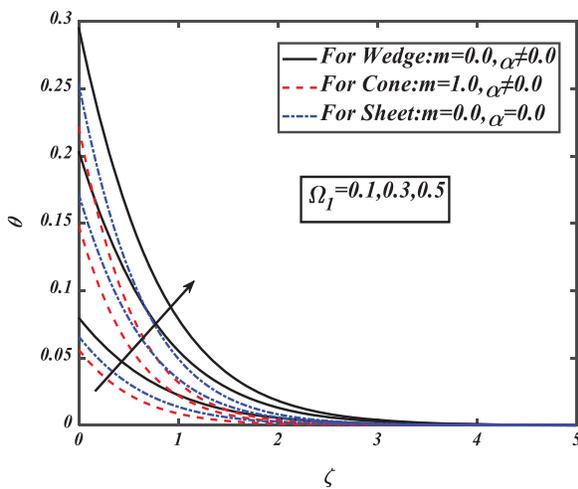
Figure 10: Pictogram of Ω_1 over θ
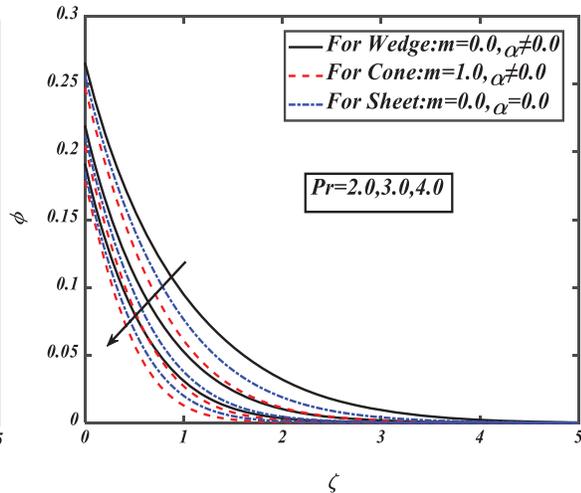
Figure 11: Pictogram of Pr over φ
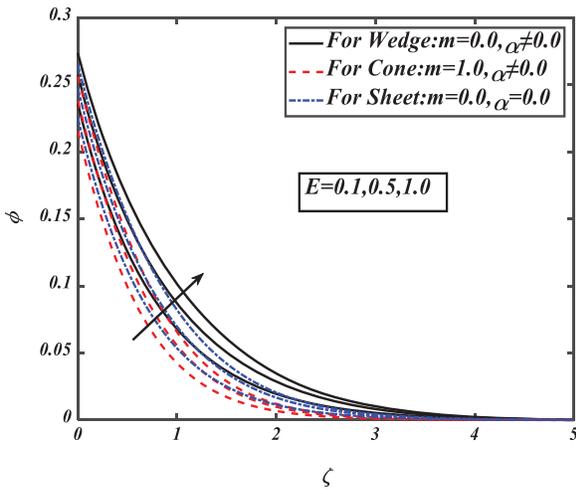
Figure 12: Pictogram of E over φ
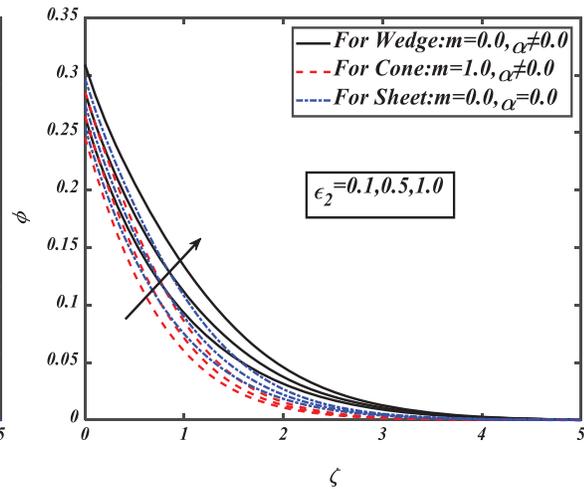
Figure 13: Pictogram of ε_2 over φ
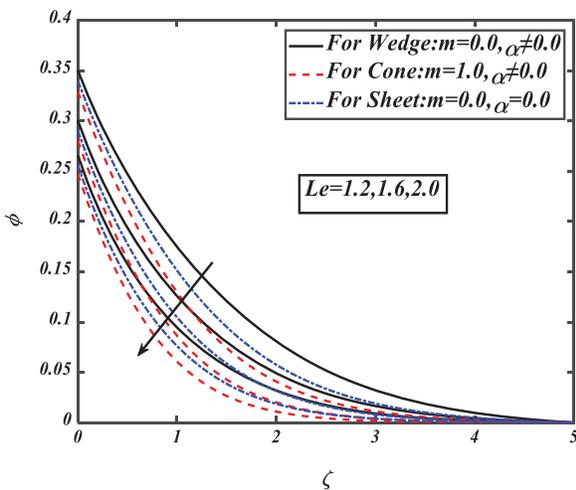
Figure 14: Pictogram of Le over φ
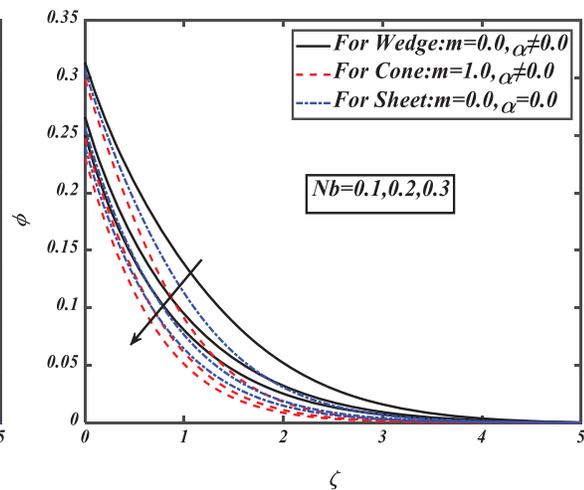
Figure 15: Pictogram of Nb over φ

Figs. 17 and 18 explain the variation of solutal Biot number Ω_2, and microorganism Biot numbers Ω_3 respectively for concentration and motile density profiles. The concentration and motile density profile depends upon the Biot number for all three conditions with respect to all three different geometries (wedge, cone and sheet). Here concentration and microorganism's field boosted for larger Biot numbers. Fig. 19 illustrates the impact of Peclet number on χ for three different geometries like wedge, cone and sheet. Largest values of Peclet number diminish the microorganism distribution. Fig. 20 illustrates that the bioconvection Lewis number Lb is a decreasing function for motile density profile χ of three geometries (wedge, cone and sheet). The χ diminished and the value of Lb are higher for the cause of increase in the diffusivity of the motile microorganism.
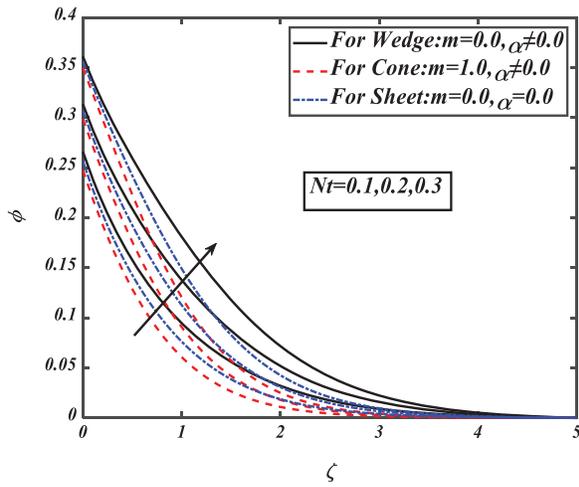
Figure 16: Pictogram of Nt over φ
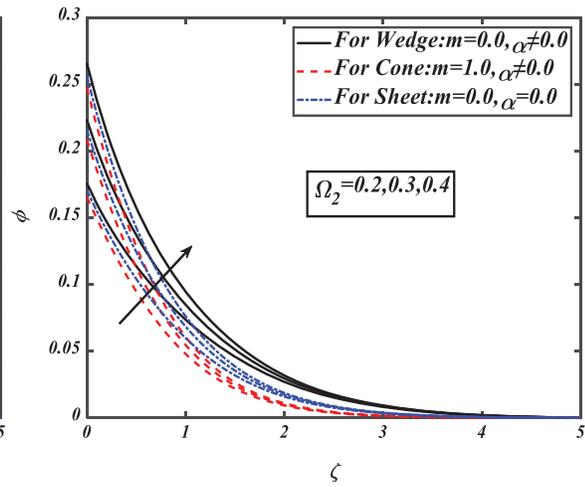
Figure 17: Pictogram of Ω_2 over φ
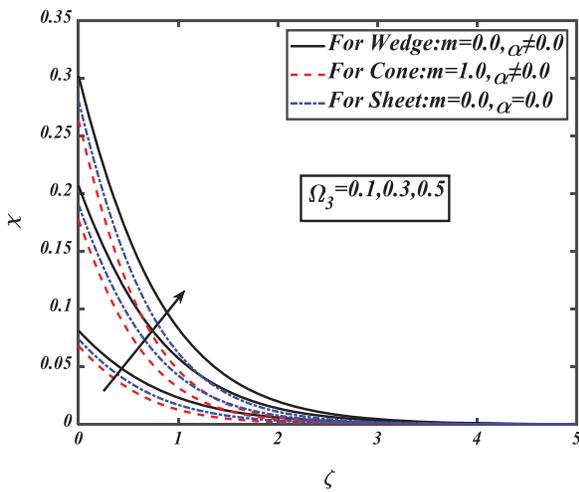
Figure 18: Pictogram of Ω_3 over χ
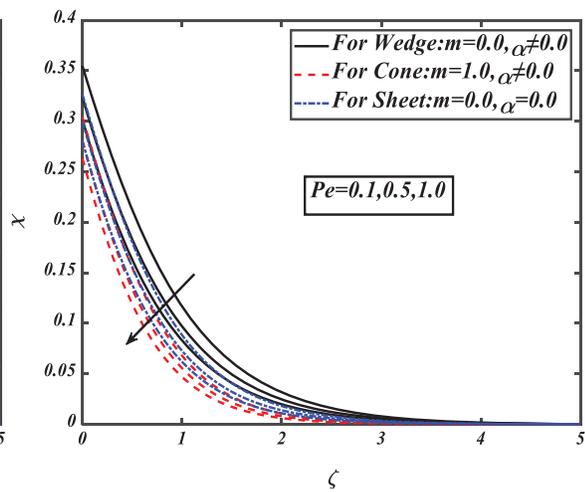
Figure 19: Pictogram of Pe over χ
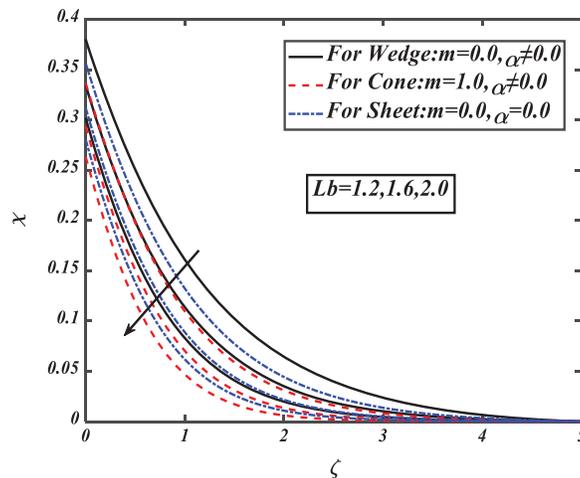
Figure 20: Pictogram of Lb over χ

5 Final Remarks

Heat and mass transformation of the nanofluid bioconvection flow under the melting mechanisms is scrutinized in the existence of cross-diffusion impacts. Mathematical modeling is fixed to scrutinize the flowing performance on vertically three different geometries (cone, wedge, and plate). Some significant remarks are synopsized below:

- Fluid exposure, the fluid velocity is highest for the flow over the plate as compared with the other two geometries (cone and wedge).
- The transformation rate of mass and heat is much better for the flow via cone than flow over the wedge.
- It is investigated that both the Brownian motion diffusion parameter and thermophoretic diffusion parameter are directly proportional to the temperature of the fluid. At the same time, concentration is directly proportional to the thermophoretic parameter but inversely proportional to the Brownian diffusion parameter.
- The temperature and concentration profile performance increased for the highest value in the thermophoretic parameter.
- The microorganisms' density is inversely proportional to the Peclet number and Lewis number.
- This study analyzed the flow characteristics of non-Newtonian fluids extended for the present mathematical model.
- Reducing the amount of melting enhanced the heat transfer rate and velocity of the fluid.

Conflicts of Interest: The authors declare that they have no conflicts of interest to report regarding the present study.

References

1. Zheng, L., Niu, J., Zhang, X., Gao, Y. (2012). MHD flow and heat transfer over a porous shrinking surface with velocity slip and temperature jump. *Mathematical and Computer Modelling, 56(5–6),* 133–144. DOI 10.1016/j.mcm.2011.11.080.
2. Chauhan, D. S., Agrawal, R. (2013). MHD flow and heat transfer in a channel bounded by a shrinking sheet and a porous medium bed: Homotopy analysis method. *International Scholarly Research Notices, 2013,* 291270. DOI 10.1155/2013/291270.
3. Attia, H. A. (2006). Unsteady MHD couette flow and heat transfer of dusty fluid with variable physical properties. *Applied Mathematics and Computation, 177(1),* 308–318. DOI 10.1016/j.amc.2005.11.010.
4. Kumar, K. G., Archana, M., Gireesha, B. J., Krishanamurthy, M. R., Rudraswamy, N. G. (2018). Cross diffusion effect on MHD mixed convection flow of nonlinear radiative heat and mass transfer of casson fluid over a vertical plate. *Results in Physics, 8,* 694–701. DOI 10.1016/j.rinp.2017.12.061.
5. Ibrahim, W., Shanker, B. (2012). Boundary-layer flow and heat transfer of nanofluid over a vertical plate with convective surface boundary condition. *Journal of Fluids Engineering, 134(8),* 081203. DOI 10.1115/1.4007075.
6. Ibrahim, W., Shanker, B. (2014). Magnetohydrodynamic boundary layer flow and heat transfer of a nanofluid over non–isothermal stretching sheet. *Journal of Heat Transfer, 136(5),* 051701. DOI 10.1115/1.4026118.
7. Ibrahim, W., Shanker, B. (2015). MHD boundary layer flow and heat transfer due to a nanofluid over an exponentially stretching non–isothermal sheet. *Journal of Nanofluids, 4(1),* 16–27. DOI 10.1166/jon.2015.1125.

8. Ibrahim, W., Makinde, O. D. (2013). The effect of double stratification on boundary–layer flow and heat transfer of nanofluid over a vertical plate. *Computers Fluids, 86,* 433–441. DOI 10.1016/j.compfluid.2013.07.029.

9. Ibrahim, W., Makinde, O. D. (2015). Double-diffusive in mixed convection and MHD stagnation point flow of nanofluid over a stretching sheet. *Journal of Nanofluids, 4(1),* 28–37. DOI 10.1166/jon.2015.1129.

10. Muhammad, T., Waqas, H., Khan, S. A., Ellahi, R., Sait, S. M. (2021). Significance of nonlinear thermal radiation in 3D eyring-powell nanofluid flow with arrhenius activation energy. *Journal of Thermal Analysis and Calorimetry, 143(2),* 929–944. DOI 10.1007/s10973-020-09459-4.

11. Waqas, H., Khan, S. A., Farooq, U., Khan, I., Alotaibi, H. et al. (2021). Melting phenomenon of non-linear radiative generalized second grade nanoliquid. *Case Studies in Thermal Engineering, 26,* 101011. DOI 10.1016/j.csite.2021.101011.

12. Danish, G. A., Imran, M., Tahir, M., Waqas, H., Asjad, M. I. et al. (2021). Effects of non-linear thermal radiation and chemical reaction on time dependent flow of williamson nanofluid with combine electrical MHD and activation energy. *Journal of Applied and Computational Mechanics, 7(2),* 546–558. DOI 10.22055/JACM.2020.35122.2568.

13. Waqas, H., Farooq, U., Naseem, R., Hussain, S., Alghamdi, M. (2021). Impact of MHD radiative flow of hybrid nanofluid over a rotating disk. *Case Studies in Thermal Engineering, 26,* 101015. DOI 10.1016/j.csite.2021.101015.

14. Mabood, F., Muhammad, T., Nayak, M. K., Waqas, H., Makinde, O. D. (2020). EMHD flow of non-newtonian nanofluids over thin needle with Robinson's condition and arrhenius pre-exponential factor law. *Physica Scripta, 95(11),* 115219. DOI 10.1088/1402-4896/abc0c3.

15. Shah, N. A., Hajizadeh, A., Zeb, M., Ahmad, S., Mahsud, Y. et al. (2018). Effect of magnetic field on double convection flow of viscous fluid over a moving vertical plate with constant temperature and general concentration by using new trend of fractional derivative. *Open Journal of Mathematical Sciences, 2(1),* 253–265. DOI 10.30538/oms2017.

16. Qi, H., Fatima, N., Waqas, H., Saeed, J. (2017). Analytical solution for the flow of a generalized oldroyd-b fluid in a circular cylinder. *Open Journal of Mathematical Sciences, 1(1),* 85–96. DOI 10.30538/oms2017.

17. Farooq, M. U., Khan, M. S., Hajizadeh, A. (2019). Flow of viscous fluid over an infinite plate with caputo-Fabrizio derivatives. *Open Journal of Mathematical Sciences, 3(1),* 115–120. DOI 10.30538/oms2017.

18. Choi, S. U., Eastman, J. A. (1995). Enhancing thermal conductivity of fluids with nanoparticles. *Proceeding of the International Mechanical Engineering Congress and Exhibition*, San Francisco.

19. Buongiorno, J. (2005). Convective transport in nanofluids. *Journal of Heat Transfer, 128(3),* 240–250. DOI 10.1115/1.2150834.

20. Kuznetsov, A. V. (2011). Nanofluid bioconvection in water–based suspensions containing nanoparticles and oxytactic microorganisms: Oscillatory instability. *Nanoscale Research Letters, 6(1),* 1–13. DOI 10.1186/1556-276X-6-100.

21. Ali, L., Liu, X., Ali, B., Mujeed, S., Abdal, S. (2019). Finite element simulation of multi-slip effects on unsteady mhd bioconvective micropolar nanofluid flow over a sheet with solutal and thermal convective boundary conditions. *Coatings, 9(12),* 842. DOI 10.3390/coatings9120842.

22. Nayak, M. K., Prakash, J., Tripathi, D., Pandey, V. S., Shaw, S. et al. (2020). 3D bioconvective multiple slip flow of chemically reactive casson nanofluid with gyrotactic micro-organisms. *Heat Transfer–Asian Research, 49(1),* 135–153. DOI 10.1002/htj.21603.

23. Khan, S. U., Waqas, H., Bhatti, M. M., Imran, M. (2020). Bioconvection in the rheology of magnetized couple stress nanofluid featuring activation energy and Wu's slip. *Journal of Non-Equilibrium Thermodynamics, 45(1),* 81–95. DOI 10.1515/jnet-2019-0049.

24. Kotha, G., Kolipaula, V. R., Rao, M. V. S., Penki, S., Chamkha, A. J. (2020). Internal heat generation on bioconvection of an MHD nanofluid flow due to gyrotactic microorganisms. *The European Physical Journal Plus, 135(7),* 1–19. DOI 10.1140/epjp/s13360-020-00606-2.

25. Al-Khaled, K., Khan, S. U., Khan, I. (2020). Chemically reactive bioconvection flow of tangent hyperbolic nanoliquid with gyrotactic microorganisms and nonlinear thermal radiation. *Heliyon, 6(1),* e03117. DOI 10.1016/j.heliyon.2019.e03117.

26. Makinde, O. D., Animasaun, I. L. (2016). Bioconvection in MHD nanofluid flow with nonlinear thermal radiation and quartic autocatalysis chemical reaction past an upper surface of a paraboloid of revolution. *International Journal of Thermal Sciences, 109,* 159–171. DOI 10.1016/j.ijthermalsci.2016.06.003.

27. Makinde, O. D., Animasaun, I. L. (2016). Thermophoresis and brownian motion effects on MHD bio-convection of nanofluid with nonlinear thermal radiation and quartic chemical reaction past an upper horizontal surface of a paraboloid of revolution. *Journal of Molecular Liquids, 221,* 733–743. DOI 10.1016/j.molliq.2016.06.047.

28. Saleem, S., Rafiq, H., Al-Qahtani, A., El-Aziz, M. A., Malik, M. Y. et al. (2019). Magneto jeffrey nanofluid bioconvection over a rotating vertical cone due to gyrotactic microorganism. *Mathematical Problems in Engineering, 2019,* 1–12. DOI 10.1155/2019/3478037.

29. Waqas, H., Khan, S. U., Hassan, M., Bhatti, M. M., Imran, M. (2019). Analysis on the bioconvection flow of modified second-grade nanofluid containing gyrotactic microorganisms and nanoparticles. *Journal of Molecular Liquids, 291,* 111231. DOI 10.1016/j.molliq.2019.111231.

30. Chu, Y. M., Waqas, H., Hussain, S., Yasmein, S., Khan, S. U. et al. (2021). Joule heating, activation energy and modified diffusion analysis for 3D slip flow of tangent hyperbolic nanofluid with gyrotactic microorganisms. *Modern Physics Letters B, 35(16),* 2150278. DOI 10.1142/S021798492150278X.

31. Waqas, H., Khan, S. A., Alghamdi, M., Alqarni, M. S., Muhammad, T. (2021). Numerical simulation for bio-convection flow of magnetized non-newtonian nanofluid due to stretching cylinder/plate with swimming motile microorganisms. *The European Physical Journal Special Topics, 230,* 1–18. DOI 10.1140/epjs/s11734-021-00041-z.

32. Waqas, H., Imran, M., Bhatti, M. M. (2021). Bioconvection aspects in non-newtonian three-dimensional carreau nanofluid flow with cattaneo-christov model and activation energy. *The European Physical Journal Special Topics, 230,* 1–14. DOI 10.1140/epjs/s11734-021-00046-8.

33. Waqas, H., Imran, M., Bhatti, M. M. (2020). Influence of bioconvection on Maxwell nanofluid flow with the swimming of motile microorganisms over a vertical rotating cylinder. *Chinese Journal of Physics, 68,* 558–577. DOI 10.1016/j.cjph.2020.10.014.

34. Song, Y. Q., Khan, S. A., Imran, M., Waqas, H., Khan, S. U. et al. (2021). Applications of modified darcy law and nonlinear thermal radiation in bioconvection flow of micropolar nanofluid over an off centered rotating disk. *Alexandria Engineering Journal, 60(5),* 4607–4618. DOI 10.1016/j.aej.2021.03.053.

35. Song, Y. Q., Waqas, H., Al-Khaled, K., Farooq, U., Khan, S. U. et al.. (2021). Bioconvection analysis for sutter by nanofluid over an axially stretched cylinder with melting heat transfer and variable thermal features: A marangoni and solutal model. *Alexandria Engineering Journal, 60(5),* 4663–4675. DOI 10.1016/j.aej.2021.03.056.

36. Waqas, H., Manzoor, U., Muhammad, T., Hussain, S. (2021). Thermo-bioconvection transport of nanofluid over an inclined stretching cylinder with cattaneo-christov double-diffusion. *Communications in Theoretical Physics, 73,* 075006. DOI 10.1088/1572-9494/abfcb9.

37. Akram, S., Razia, A. (2021). Hybrid effects of thermal and concentration convection on peristaltic flow of fourth grade nanofluids in an inclined tapered channel: Applications of double-Diffusivity. *Computer Modeling in Engineering & Sciences, 127(3),* 901–922. DOI 10.32604/cmes.2021.014469.

38. Ejaz, A., Abbas, I., Nawaz, Y., Arif, M. S., Shatanawi, W. et al. (2020). Thermal analysis of MHD non–newtonian nanofluids over a porous media. *Computer Modeling in Engineering & Sciences, 125(3),* 1119–1134. DOI 10.32604/cmes.2020.012091.

39. Vajravelu, K., Nayfeh, J. (1992). Hydromagnetic convection at a cone and a wedge. *International Communications in Heat and Mass Transfer, 19(5),* 701–710. DOI 10.1016/0735-1933(92)90052-J.

40. Chamkha, A. J. (1996). Non-darcy hydromagnetic free convection from a cone and a wedge in porous media. *International Communications in Heat and Mass Transfer, 23(6),* 875–887. DOI 10.1016/0735-1933(96)00070-X.

41. Khan, M. S., Karim, I., Islam, M. S., Wahiduzzaman, M. (2014). MHD boundary layer radiative, heat generating and chemical reacting flow past a wedge moving in a nanofluid. *Nano Convergence, 1(1),* 1–13. DOI 10.1186/s40580-014-0020-8.

42. Abd El-Aziz, M. (2008). Thermal-diffusion and diffusion-thermo effects on combined heat and mass transfer by hydromagnetic three-dimensional free convection over a permeable stretching surface with radiation. *Physics Letters A, 372(3),* 263–272. DOI 10.1016/j.physleta.2007.07.015.

43. Eckert, E. R. G., Drake, R. M. (1971). *Analysis of heat and mass transfer.* USA: McGraw-Hill.

44. Mortimer, R. G., Eyring, H. (1980). Elementary transition state theory of the soret and dufour effects. *Proceedings of the National Academy of Sciences, 77(4),* 1728–1731. DOI 10.1073/pnas.77.4.1728.

45. Devi, S. A., Devi, R. U. (2011). Soret and dufour effects on MHD slip flow with thermal radiation over a porous rotating infinite disk. *Communications in Nonlinear Science and Numerical Simulation, 16(4),* 1917–1930. DOI 10.1016/j.cnsns.2010.08.020.

46. Rafiq, T., Mustafa, M., Farooq, M. A. (2020). Modeling heat transfer in fluid flow near a decelerating rotating disk with variable fluid properties. *International Communications in Heat and Mass Transfer, 116,* 104673. DOI 10.1016/j.icheatmasstransfer.2020.104673.

47. Raju, C. S. K., Sandeep, N. (2016). Falkner-skan flow of a magnetic-Carreau fluid past a wedge in the presence of cross diffusion effects. *The European Physical Journal Plus, 131(8),* 1–13. DOI 10.1140/epjp/i2016-16267-3.

48. Waqas, M., Hayat, T., Alsaedi, A., Khan, W. A. (2020). Analytical evaluation of oldroyd-B nanoliquid under thermo-solutal robin conditions and stratifications. *Computer Methods and Programs in Biomedicine, 196,* 105474. DOI 10.1016/j.cmpb.2020.105474.